Droplet Cooling of Heated Surfaces: Experimental and Numerical Analysis

Paolo Tartarini*, Mauro A. Corticelli and Paolo E. Santangelo
Dipartimento di Ingegneria Meccanica e Civile (DIMeC),
Università degli Studi di Modena e Reggio Emilia, Via Vignolese 905/b, 41100 Modena, Italy

Abstract

The present work is focused on measuring the transient contact temperature between a droplet and a hot solid surface. Experimental tests have been carried out employing infrared thermography. Droplets of bidistilled and deionized water have been gently deposited by a precision syringe onto the upper surface of a heated disk. This latter consists of a Barium Fluoride (BaF_2) disk, having high transmittance (about 90%) in the 8-12 μm range (typical of long-wave infrared cameras). The interface temperature has been measured from below through the solid material by an infrared thermocamera. As far as the solid can be assumed as infrared-transparent, a black coating layer has been applied to allow radiative heating of the solid surface. The bottom surface temperature of the coating is undistinguishable from the solid-liquid interface temperature and has been monitored. Single-phase evaporation regime has been analyzed in detail. A numerical code is then presented, which simulates evaporation process of water droplets on hot solid surfaces. The three-dimensional energy-diffusion equation is discretized by the finite volume method and is employed to model the transient temperature within both the droplet and the solid substrate. In this stage of development, the code simulates the substrate cooling effect due to a droplet in single-phase evaporation regime; however, its applicability to nucleate boiling and film boiling regimes can be considered as reasonably possible. The code is implemented in Matlab®, using a modular and flexible architecture. As a final task, numerical results are validated through a comparison with the experimental data.

Introduction

Many engineering and safety applications require that a hot surface is effectively cooled down by a spray of water droplets. Fire suppression in nuclear power plants, in process chemical storage and in fuel storage facilities is a primary application which has inspired a number of experimental and theoretical studies on the phenomena associated with spray cooling. Only some examples of important contributions will be mentioned here among the numerous available in the scientific literature. Fire protection applications are the focus of the present work, that lies in the frame of a long-term research: its results have been published in some papers during almost two decades [1-8]. The behavior of sessile droplets has been investigated extensively by several researchers. Some fundamental studies on heat-transfer modeling for sprays are presented in [9-13]. These works mainly deal with film-boiling regime. Gorton [9] found experimentally that the vapor-film thickness between a sessile droplet and the surface increases, while the heat-transfer coefficient decreases with an increase of surface temperature. Wachters et al. [10] proposed a detailed discussion of the shape of a sessile drop on a horizontal hot solid surface. Baumeister et al. [11] developed a dimensionless correlation for vaporization time of discrete liquid masses. Bolle and Moureau [12] and Chandra and Avedisian [13] presented analytical methods to predict the thickness of the vapor layer separating a hemispherical liquid droplet from a hot surface. Also the behavior of impinging droplets has been investigated by many researchers. Impact and deformation of a liquid droplet impinging upon a heated surface has been studied with extensive use of high speed photography. Among the early works, Wachters and Westerling [14] observed that impact and breakup of water droplets striking a horizontal surface at 400°C (film-boiling regime) could be grouped into three general categories depending upon the droplet Weber number (ratio between droplet inertial forces and surface-tension forces). In the low Weber number regime ($We<30$), Wachters and Westerling [14] observed that the droplet spread out radially upon impact into a flat disk with a fairly uniform thickness, and the impact did not affect its initial shape. During an evaporative transient (single-phase evaporation) the radius of the wetted region remains constant and the solid-liquid contact angle decreases until a minimum critical value (receding angle) is reached. Detailed information on the receding angle is available in several works [15-18]. As the droplet is completely evaporated the solid-surface temperature tends to return to its initial value. In the mid-Weber-number regime ($30<We\leq80$), the droplet was observed to split into a large globule and a small satellite. Finally, in the high Weber-number regime

*Corresponding author

(We>80), the droplet began to spread out radially upon impact into a flat disk: its rim broke into several small droplets, which quickly dispersed away. The flat disk itself then broke up violently into many small droplets. The classification by Wachters and Westerling [14] is usually accepted at high solid-surface temperatures; however, the droplet-impact characteristics are found to be strongly dependent on temperature over the ranges including single-phase evaporation and nucleate boiling phenomena. Chandra and Avedisian [13] investigated the influence of surface temperature on droplet impact dynamics through a photographic analysis. They observed spreading structure and rate of the liquid film, vapor bubble formation and contact angle for *n*-heptane droplets with We = 43 impinging upon a polished stainless-steel surface. They showed that all these impact characteristics were highly temperature-dependent over the range between 24 and 250 °C. The observations of Wachters and Westerling [14] in the field of high temperatures were confirmed later by Bolle and Moureau [12], who employed high-speed film-based photography to investigate droplet impact for surface temperature in the range of 800-1200 °C (film-boiling regime) and *We* between 1 and 1500. Extensive contributions in this field are also available in Bernardin and Mudawar [19] and Bernardin et al. [20]. Recent improvements of photographic techniques allowed some authors to obtain excellent results in terms of droplet-impact visualization. In terms of solid heating modes, when the solid surface is heated by conduction from below, the solid layer under the droplet acts as a heat source, while it can be assumed as a heat sink when the solid surface is heated by radiation from above. Moreover, in case of significant radiative heating, droplets absorb heat directly from ambient, and their surface tension strongly decreases. The two described scenarios are certainly of some interest for industrial and civil-engineering applications.

Experimental Apparatus and Results

A new method is proposed to measure the interface temperature without contact, in order to overcome possible difficulties in measuring the liquid-solid interface temperature without using direct-contact sensors. Droplets are released onto a heated solid surface of a material, that is transparent in the infrared spectral band. Therefore, the experimental apparatus was built to measure the temperature at the solid-liquid interface during evaporation of liquid droplets. The horizontal solid surface is heated by radiation from above. The interface temperature is measured from below, through the solid material, by infrared thermography. Since the solid is infrared (IR)-transparent, a coating layer is used to allow radiative heating of the solid surface and provide a method to visualize the bottom surface temperature, that is *de facto* undistinguishable from the solid-liquid interface temperature. A sketch of the test section is reported in Fig. 1. The full experimental apparatus and setup is thoroughly described in Tarozzi et al. [7,8]. The IR-transparent material is Barium Fluoride (BaF_2) with a diameter of 75 mm and a thickness of 3 mm, which is mounted on a horizontal slab of insulating material.

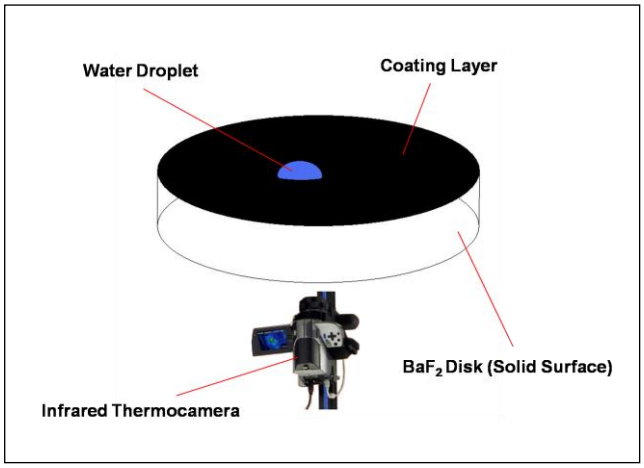

Figure 1. Sketch of the test section (not to scale).

A circular window is opened through the slab and is filled by the transparent disk in order to avoid radial heat losses and provide homogeneous heating of the BaF_2 disk. Droplets of bidistilled and deionized water are gently deposited (the Weber number is always lower than 30) by a precision syringe onto the upper surface of the heated disk. The top surfaces of both disk and slab are heated from above by four radiant panels; the heating is active during the deposition of the droplets and the entire evaporation period. The panels are fed by a three-phase power supply which is controlled on a temperature feedback by a Variac. This feature allows to modulate the radiant flux and, therefore, the initial surface temperature by varying the applied voltage. A homogeneous irradiation is achieved by modifying the position of each panel independently. A uniform heating was easily achieved during the tests. The temperature uniformity of the test section has been verified by means of thermographic images. The main component of the apparatus is the BaF_2 disk, that is transparent in the infrared spectral band: due to this feature, a coating layer has to be used to provide radiative heating of the solid surface. Thanks to the structure of this coating layer, the solid-liquid interface temperature can be measured. In fact, the infrared camera measures the temperature of the bottom surface of the coating layer through the transparent disk (i.e.: at the coating-solid interface). However, this can be assumed to be equal to the solid-liquid interface temperature if the coating layer is thin and conductive enough.

The interface temperature is measured from below, through the solid material, by an Avio TVS-500 thermographic camera, carrying a micro-bolometric FPA sensor which operates in the long-wave spectral range (8-12 μm). The camera features an IEEE-1394 interface, which allows to operate at up to 60 frames per second. Calibration is automatically performed by the instrument itself. The infrared frame sequences are then processed by a Matlab® post-processor, in order to enhance the image quality by noise filtering and emissivity maps. Figure 2 reports four frames of a sequence of the evaporation of four distinct droplets (50 μl each) on the BaF_2 disk at initial temperature of 90 ± 1 °C. The image resolution consists of a ratio 1 pixel to 152 μm.

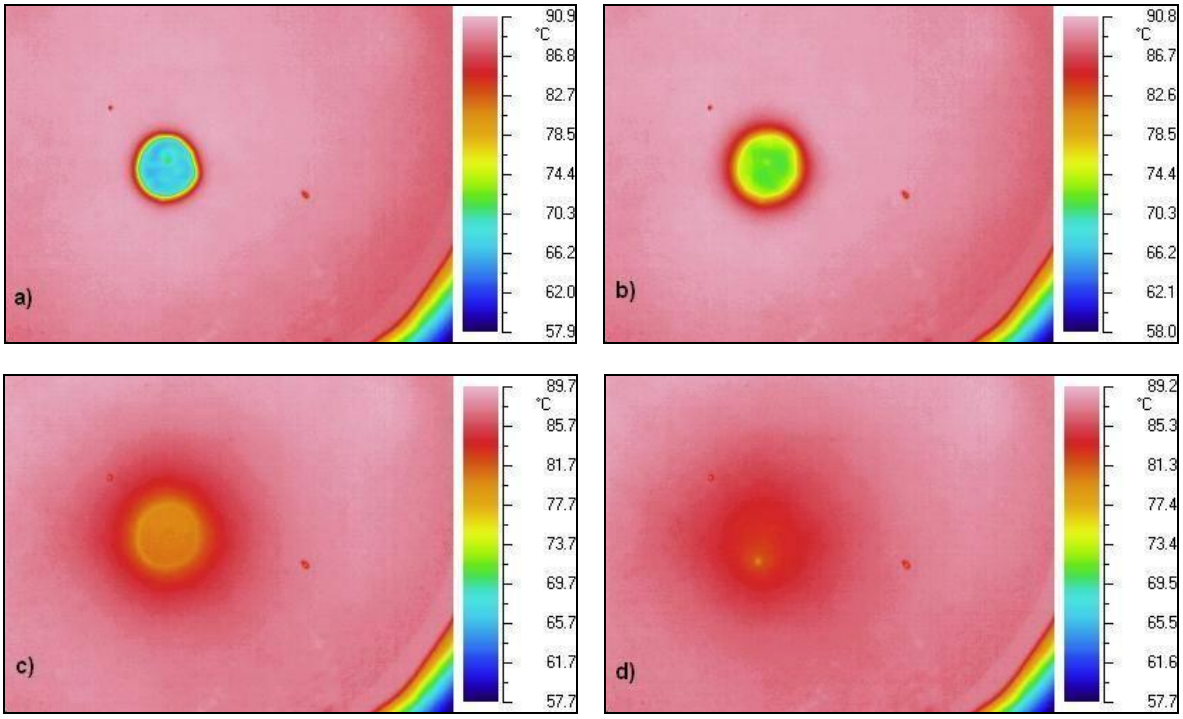

Figure 2. Thermographic images of the droplet-evaporation process: a) deposition; b) 1 s after deposition; c) 10 s after deposition; d) last image before complete evaporation (162 s).

Numerical Approach and Results

In previous attempts of modeling single-phase droplet cooling, the work by Rizza [21], di Marzo et al. [3] and Tartarini and di Marzo [4] demonstrated that conduction is the dominant heat transfer mode inside the droplets in the low superheat regime. After carrying out extensive experimental researches, a numerical code is formulated to predict evaporative cooling of solid surfaces induced by a gently deposited water droplet. The code was based on a solid-liquid coupled model, that predicted the droplet evaporation and the solid-surface cooling for materials with thermal conductivity spanning over more than two orders of magnitude. The numerical solution of the conduction equation connects a Control-Volume Method (CVM), used for the liquid, to a Boundary-Element Method (BEM, as in Wrobel and Brebbia [22]), used for the solid. The numerical predictions by that code showed very good agreement with experimental data in terms of both evaporation times (lifetimes) and solid-surface temperatures. That code was very effective, but it could not simulate the three-dimensional behavior of evaporative cooling at higher superheat regimes.

A new numerical code is here presented, that simulates evaporation of water droplets on hot solid surfaces. The three-dimensional energy-diffusion equation is discretized using the finite-volume method and is employed to model the transient within both the droplets and the solid substrate. At this stage of development, the new code is capable of simulating the substrate cooling effect due to a droplet in single-phase evaporation regime only, but its structure allows an easy extension to nucleate-boiling and film-boiling regimes. The code is implemented in Matlab®, using a modular and flexible architecture.

The thermal behavior of both liquid droplets and solid substrate is described by the Fourier equation of heat diffusion:

$$\frac{\partial T_l}{\partial t} = \alpha_l \nabla^2 T_l, \qquad (1)$$

$$\frac{\partial T_s}{\partial t} = \alpha_s \nabla^2 T_s. \qquad (2)$$

The vapor mass flux *m''* at the liquid-air interface can be estimated by the classical correlation due to Chilton and Colburn [23]:

$$m'' = 0.624 \cdot h \cdot \left(\frac{d_{aw}}{\alpha_a}\right)^{\frac{2}{3}} \frac{1}{c_a} \frac{p_{sat@T_l} - \varphi p_{sat@T_a}}{p - p_{sat@T_l}}, \qquad (3)$$

where the convection coefficient *h* can be evaluated from common relationships available in the scientific literature.

Due to the evaporative mass flux, the following boundary condition can be imposed on the heat flux across the liquid-air interface:

$$k_l \frac{\partial T_l}{\partial n} = h(T_l - T_a) + m''\Lambda_l - q''_{rad}. \qquad (4)$$

The conditions on the top surface of the solid outside the droplet and on the bottom surface are:

$$k_s \frac{\partial T_s}{\partial z} = h(T_s - T_a) - q''_{rad}. \qquad (5)$$

In the present configuration, the vertical surfaces of the solid are considered adiabatic; in particular, two surfaces are symmetry planes. The boundary conditions at the solid-liquid interface state continuity of temperature and heat flux:

$$T_l = T_s, \qquad (6)$$

$$k_l \frac{\partial T_l}{\partial z} = k_s \frac{\partial T_s}{\partial z}. \qquad (7)$$

The spherical-cap-shaped droplet is initially symmetrical with respect to the vertical axis, that is perpendicular to the surface of the substrate. The described 3D model has been coded in Matlab® to obtain a transient temperature profile on the substrate surface, that could be compared with the thermographic experimental data. A structured non-uniform mesh is used, which is refined where the strongest temperature gradients and largest heat fluxes are expected (i.e.: at the interfaces and below the droplet). The elements in the droplet have different height, to consider the spherical-cap geometry.

The governing equations for the liquid and the solid substrate are discretized by finite volumes, with a Crank-Nicolson algorithm for the time-advancement. An explicit approach is used to evaluate the liquid loss due to evaporation, as well as the heat transfer coefficient and the material properties at each node and time step. In particular, at every time step, the evaporated mass flux at the liquid-air interface is calculated for every top cell area, and the droplet is built and meshed again, considering the new amount of non-evaporated liquid. The difference between the initial droplet volume and the reconstructed volume is less than -0.0014421%.

Some preliminary results for single droplet evaporative transients are reported in Figs. 3-6. In these figures, the calculated temperature of the lower coating surface and of the upper surface of the BaF_2 disk are plotted versus time (Fig. 3) or radial distance (Figs. 4-5) during different evaporative transients, and the numerical predictions are compared with the corresponding data from experimental measurements.

Figure 3 reports a comparison between experimental data and numerical predictions for the temperature transient of a solid surface point very close to the droplet center. Both experimental data and numerical calculations stress out the sudden

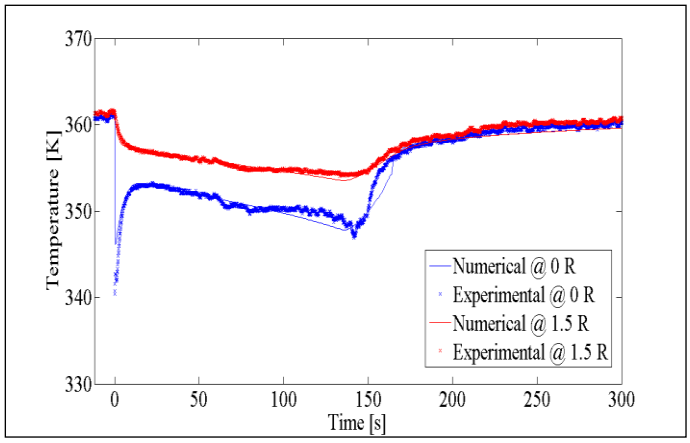

Figure 3. Temperature vs. Time at different radial locations *x* (center of the droplet and 1.5 droplet radius), at two different times after droplet deposition: comparison between experimental and numerical results.

temperature decrease right after the droplet deposition; the code predictions tend to overestimate the solid surface temperature evolution immediately after the droplet deposition, but during the following portion of the transient the temperature evolution is well predicted.

Figures 4 and 5 report the comparisons between experimental data and numerical predictions for the solid surface temperature distribution along the radial coordinate from the droplet center. In the challenging zone of the wetted area, the same discrepancies observed in Fig. 3 affect the Temperature vs. Radial Coordinate plots of Figs. 4-5. In particular, the code tends to overestimate the temperature in the central zone of the droplet during the first instants of evaporation (Fig. 4); in the remaining part of the transient (Fig. 5), a better agreement is evident even if at the edge of the droplet the measured temperatures are lower than the predicted ones. The agreement appears to be satisfactory.

Figure 6 shows the behavior of the contact angle as it is computationally modeled. It decreases from the initial deposition angle (about 43°) to the final receding angle (about 5°) in less than 140 s. As the receding angle is reached, it holds for the remaining 25 s, until the complete collapse of the droplet.

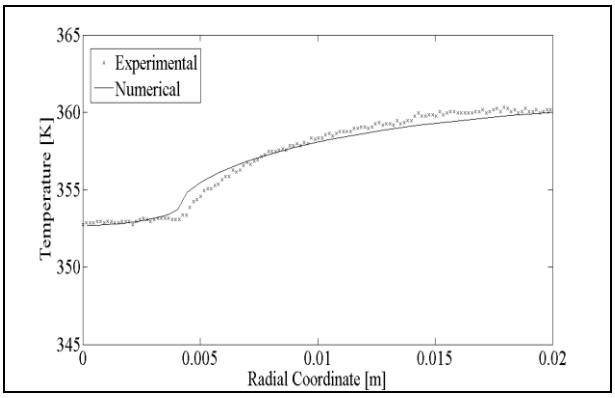

Figure 4. Temperature vs. Radial Coordinate at 5 s after droplet deposition: comparison between experimental and numerical results.

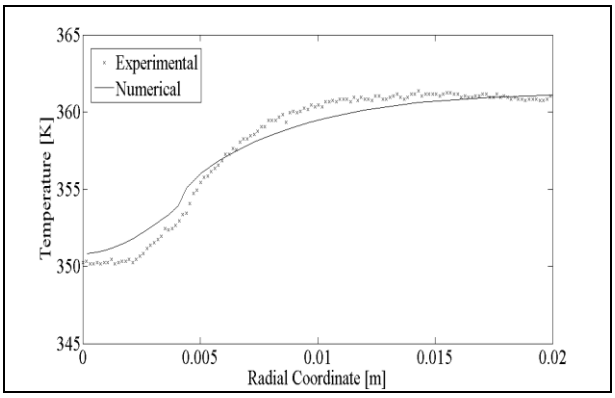

Figure 5. Temperature vs. Radial Coordinate at 30 s after droplet deposition: comparison between experimental and numerical results.

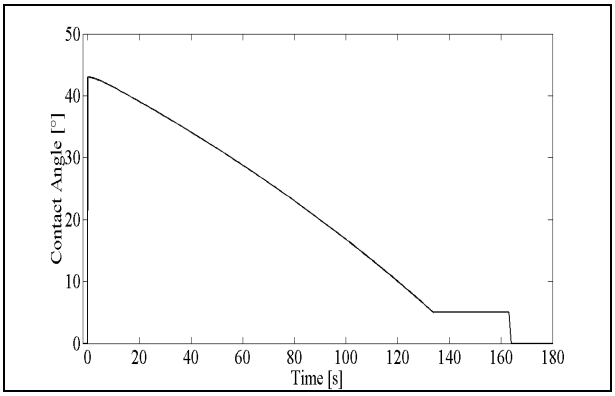

Figure 6. Temporal evolution of the droplet contact angle as modeled in the numerical code

Concluding remarks

An approach to non-intrusive measurement of the transient contact temperature between impinging droplets and hot solid surfaces is presented. The solid-liquid interface temperature has been monitored from below through an IR- transparent material. That material had been coated with a very thin layer of high-emissivity and opaque paint on its upper side, so that it could effectively respond to the infrared camera located below. The experimental results related to transient-temperature distribution confirmed many typical trends of dropwise cooling. The direct observation of the solid-liquid interface temperature enhanced the comprehension of the interactions between droplets and hot surfaces. A numerical code has been developed and proposed to simulate the evaporation of water droplets on hot solid surfaces. At the present stage of development, only single-phase evaporation has been addressed. The three-dimensional energy-diffusion equation is discretized using the finite-volume method and has been employed to model the transient within both the droplets and the solid substrate. The numerical results have been compared with the experimental data. A good agreement is generally showed. Moreover, the present contribution may also be considered a starting point to perform simulations on multi-droplet systems, which are of strong interest for many practical applications. Nucleate boiling within the droplet and high Weber numbers will be progressively included into the numerical simulation.

Acknowledgments

These studies were made possible by the financial contribution of the Italian M.I.U.R. All the students who worked at the experimental apparatus during the entire period of the present research are also acknowledged.

Nomenclature

d_{aw}	air-water mass diffusivity ($m^2\ s^{-1}$)
k	thermal conductivity ($W\ m^{-1}\ K^{-1}$)
h	heat transfer coefficient ($w\ m^{-2}\ K^{-1}$)
m''	vapor mass flux ($kg\ s^{-1}\ m^{-2}$)
n	normal coordinate (m)
p	pressure (Pa)
q''	heat flux ($W\ m^{-2}$)
R	droplet (wetted area) radius (m)
T	temperature (°C or K)
t	time (s)
x	radial coordinate from the droplet center (mm)
z	vertical coordinate (m)

Greek letters

α	thermal diffusivity ($m^2\ s^{-1}$)
θ	solid-liquid contact angle (rad)
Λ	latent heat of vaporization ($J\ kg^{-1}$)
φ	relative humidity

Subscripts

0	initial
a	air, ambient
l	liquid
rad	radiative
s	solid
sat	saturation

References

1. di Marzo, M., and Evans, D., *J. Heat Transf. – Trans. ASME* 111:210-213 (1989).
2. di Marzo, M., Tartarini, P., Liao, Y., Evans, D., and Baum, H., *ASME HTD* 166:51-58 (1991).
3. di Marzo, M., Tartarini, P., Liao, Y., Evans, D., and Baum, H., *Int. J. Heat Mass Transf.* 36:4133-4139 (1993).
4. Tartarini, P., and di Marzo, M., *Advanced Computational Methods in Heat Transfer III*, Editors: Wrobel, L.C., Brebbia, C.A., and Nowak, A.J., Computer Mechanics Publications, 1994, pp. 473-480.
5. Chandra, S., di Marzo, M., Qiao, Y.M., and Tartarini, P., *Fire Saf. J.* 27:141-158 (1996).
6. Tartarini, P., Lorenzini, G., Randi, M.R., and di Marzo, M., *Fourth World Conference on Experimental Heat Transfer, Fluid Mechanics and Thermodynamics*, Brussels, Belgium, 1997, pp. 1319-1326.
7. Tarozzi, L., Muscio, A., and Tartarini, P., *XXIII UIT National Heat Transfer Conference*, Parma, Italy, June 2005, pp. 269-274.
8. Tarozzi, L., Muscio, A., and Tartarini, P., *Exp. Therm. Fluid Sci.* 31:857-865 (2007).
9. Gorton, C.W., Ph.D. Thesis, Purdue University, West Lafayette, IN, USA, 1953.
10. Wachters, L.H.J., Bonne, H., and Van Nouhuis, H.J., *Chem. Eng. Sci.* 21:923-936 (1966).
11. Baumeister, K.J., Hamill, T.D., Schwartz, F.L., and Schoessow, G.J., *Chem. Eng. Prog.* 62:52-61 (1973).
12. Bolle, L., and Moureau, J.C., Spray Cooling of Hot Surfaces, Editors: Hewitt, G.F., Delhaye, J.M., and Zuber, N., *Multiphase Science and Technology*, Hemisphere, 1976, pp. 1-92.
13. Chandra, S., and Avedisian, C.T., *Proc. R. Soc.* 432:13-41 (1991).
14. Wachters, L.H.J., and Westerling, N.A.J., *Chem. Eng. Sci.* 21:1047-1056 (1966).
15. Adam, N., and Jessop, G., *J. Chem. Soc*. 127:1863-1868 (1925).
16. Good, R.J., *J. Colloid Interface Sci.* 74:5041-5042 (1952).
17. Herzberg, W.J., and Marian, J.E., *J. Colloid Interface Sci.* 33:161-163 (1970).
18. Herzberg, W.J., Marian, J.E., and Vermeulen, T., *J. Colloid Interface Sci.* 33:164-171 (1970).
19. Bernardin, J.D., and Mudawar, I., *Int. J. Heat Mass Transf.* 40:2579-2593 (1997).
20. Bernardin, J.D., Stebbins, C.J., and Mudawar, I., *Int. J. Heat Mass Transf.* 40:247-267 (1997).
21. Rizza, J.J., *J. Heat Transf. – Trans. ASME* 103:501-507 (1981).
22. Wrobel, L.C., and Brebbia, C.A., *Int. J. Heat Mass Transf.* 24:843-850 (1981).
23. Chilton, T.H., and Colburn, A.P., *Ind. Eng. Chem. Res.* 26:1183-1187 (1934).